https://doi.org/10.5194/egusphere-2025-2204
Preprint. Discussion started: 28 May 2025

Long–term Trends in $PM_{2.5}$ Chemical Composition and Its Impact on Aerosol Properties: Field Observations from 2007 to 2020 in Pearl River Delta, South China

Yunfeng He [1, 4], Xiang Ding [1, 2, 3], Quanfu He [8], Yuqing Zhang [9], Duohong Chen [10], Tao Zhang [10], Kong Yang [1, 4], Junqi Wang [1, 4], Qian Cheng [1, 4], Hao Jiang [1, 4], Zirui Wang [1, 4], Ping Liu [1, 4], Xinming Wang [1, 2, 3], Michael Boy [5, 6, 7]

[1]State Key Laboratory of Advanced Environmental Technology, Guangzhou Institute of Geochemistry, Chinese Academy of Sciences, Guangzhou 510640, China
[2]Guangdong–Hong Kong–Macao Joint Laboratory for Environmental Pollution and Control, Guangzhou Institute of Geochemistry, Chinese Academy of Science, Guangzhou 510640, China
[3]Guangdong Key Laboratory of Environmental Protection and Resources Utilization, Guangzhou Institute of Geochemistry, Guangzhou 510640, China
[4]University of Chinese Academy of Sciences, Beijing 100049, China
[5]Institute for Atmospheric and Earth Systems Research, University of Helsinki, Helsinki 00014, Finland
[6]Atmospheric Modelling Centre – Lahti, Lahti University Campus, Lahti 15140, Finland
[7]School of Energy Systems, Lappeenranta-Lahti University of Technology, Lappeenranta 53850, Finland
[8]Thrust of Earth, Ocean and Atmospheric Sciences, The Hong Kong University of Science and Technology (Guangzhou), Guangzhou 511453, China
[9]School of Environment and Safety Engineering, North University of China, Taiyuan 030051, China
[10]State Environmental Protection Key Laboratory of Regional Air Quality Monitoring, Guangdong Environmental Monitoring Center, Guangzhou 510308, China

Correspondence to: Xiang Ding (xiangd@gig.ac.cn), Michael Boy (michael.boy@helsinki.fi)

https://doi.org/10.5194/egusphere-2025-2204
Preprint. Discussion started: 28 May 2025

Abstract

Long–term data on $PM_{2.5}$ chemical composition provide essential information for evaluating the effectiveness of air pollution control measures and understanding the evolving mechanisms of secondary species formation in the real atmosphere. This study presented field measurements of $PM_{2.5}$ and its chemical composition at a regional background site in the Pearl River Delta (PRD) from 2007 to 2020. $PM_{2.5}$ concentration declined significantly from 87.1 ± 15.5 μg m^{-3} to 34.0 ± 11.3 μg m^{-3} (–4.0 μg m^{-3} yr^{-1}). The proportion of secondary species increased from 57% to 73% with the improvement in air quality. Among these species, sulfate (SO_4^{2-}) showed a sharp decline, while nitrate (NO_3^-) exhibited a moderate decrease. Consequently, the proportion of NO_3^- in 2020 doubled relative to 2007. In addition, we further found that SO_4^{2-} reduction (–10% yr^{-1}) lagged behind SO_2 reduction (–13% yr^{-1}), while NO_3^- reduction (–6% yr^{-1}) outpaced that of NO_2 (–3% yr^{-1}). These contrasting trends were associated with an increase in sulfur oxidation rate (SOR) and a decrease in nitrogen oxidation rate (NOR). Changes in $PM_{2.5}$ chemical composition also influenced aerosol physicochemical properties, such as aerosol pH (0.06 yr^{-1}), aerosol liquid water content (ALWC, –1.1 μg m^{-3} yr^{-1}), and the light extinction coefficient (b_{ext}, –21.44 Mm^{-1} yr^{-1}). Given important roles of aerosol acidity and ALWC in the heterogeneous reactions, these changes may further inhibit the formation of secondary species in the atmosphere, particularly SOA.

https://doi.org/10.5194/egusphere-2025-2204
Preprint. Discussion started: 28 May 2025

1. Introduction

Ambient fine particulate matter ($PM_{2.5}$) is a major air pollutant with significant implications for global climate, air quality, and human health (Burnett et al., 2018; Chen et al., 2021; Ding et al., 2021; Pye et al., 2021; Vohra et al., 2022). $PM_{2.5}$ comprises a complex mixture of primary and secondary components. Primary components, including primary organic aerosol (POA), elemental carbon (EC), and metal ions (e.g., K^+, Ca^{2+}, Na^+, Mg^{2+}), are mostly emitted from anthropogenic activities. Secondary components, such as secondary organic aerosols (SOA) and secondary inorganic aerosols (SIA; i.e., SO_4^{2-}, NO_3^-, NH_4^+), are formed through oxidation of gaseous pollutants (SO_2, NO_x, and VOCs, etc.) and partition processes. China experienced rapid economic growth and urbanization in the past decades. To address severe air pollution, the Chinese government issued the Air Pollution Prevention and Control Action Plan in 2013 (Geng et al., 2024). As a result, the chemical composition of $PM_{2.5}$ over China changed significantly (Geng et al., 2019). This change has an important impact on aerosol acidity, ALWC, and light extinction (Nguyen et al., 2016; Pye et al., 2020; Liu et al., 2022).

Acidity, defined as pH, is a crucial aerosol property that affects human health, ecosystems and climate (Nenes et al., 2020; Su et al., 2020; Song et al., 2024). Low pH increases solubility of metals associated with mineral dust (Fang et al., 2017). Previous epidemiological studies revealed that exposure to acidic $PM_{2.5}$ is relevant to high mortality and morbidity (Gwynn et al., 2000; Zhang et al., 2022a). Additionally, aerosol acidity and ALWC regulate the gas–particle partitioning of semi–volatile gases, as well as chemical reaction rates in the atmosphere, highlighting their importance for the atmospheric lifetime of pollutants (Pye et al., 2020; Nenes et al., 2021). Aqueous uptake is an important pathway for formation of secondary species (Liu et al., 2021; Yu et al., 2005; Kawamura and Bikkina, 2016). As an abundant medium, ALWC can enhance their formation (Zheng et al., 2015; Carlton and Turpin, 2013). By modifying particle ability to be activated into cloud condensation nuclei (CCN), ALWC can further influence the climate system (Duan et al., 2019). Therefore, it is necessary to explore the trends of pH and ALWC under the change in $PM_{2.5}$ chemical composition.

Aerosol pH and ALWC are determined by the presence of acidic components (i.e., SO_4^{2-} and NO_3^-), alkaline components (i.e., NH_4^+) (Seinfeld et al., 1998), and meteorological parameters, such as temperature and relative humidity. (Wang et al., 2022a). However, aerosol acidity is more responsive to dominant chemical species rather than meteorological conditions (Wu et al., 2023). According to sensitivity tests, T-H_2SO_4 (SO_2 + SO_4^{2-}) and T-NH_3 (NH_3 + NH_4^+) have the most dominant negative and positive contribution to pH variation, respectively (Wu et al., 2023). The aerosol pH exhibited noticeable spatial heterogeneity. For example, the pH values in North China (e.g., Beijing (3.0–4.9), Zhengzhou (4.5), Anyang (4.8)) (Liu et al., 2017; Wang et al., 2020) were generally higher than those in South China (e.g., Guangzhou (-0.04–0.81), Shanghai (3.06–3.30), South China Sea (1.7)) (Wang et al., 2022a; Zhou et al., 2022; Fu et al., 2015). This could result from the fact that SO_4^{2-}

https://doi.org/10.5194/egusphere-2025-2204
Preprint. Discussion started: 28 May 2025

fraction was higher in southern China (Geng et al., 2017; Liu et al., 2023) and high NH_3 emissions in northern China (Liu et al., 2023). Zhou et al. (2022) reported a downward trend of pH (from 3.33 to 3.06) at a rate of –0.24 yr^{-1} in the Yangtze River Delta (YRD) from 2011 to 2019. Conversely, Fu et al. (2015) reported an upward trend of pH (from –0.30 to 0.81) in the PRD during 2007–2012. However, this study did not cover the post–2013 period, a key period for air quality improvement.

$PM_{2.5}$ composition also affects atmospheric visibility through light scattering and absorption. Light scattering is dominated by hydrophilic components, such as organic mass (OM), $(NH_4)_2SO_4$, and NH_4NO_3, while light absorption is largely driven by light–absorbing carbon (Wang et al., 2012). The Interagency Monitoring of Protected Visual Environments (IMPROVE) algorithm, developed by the U.S. Environmental Protection Agency (EPA), is a widely used tool for estimating the light extinction coefficient (b_{ext}) (Epa, 2011). However, scattering/absorbing efficiency (MSE/MAE) employed in the IMPROVE algorithm is an approximation and simplification based on measurements of clean areas. The hygroscopic growth factor (f(RH)), which has been suggested to depend on secondary inorganic fractions (e.g., sulfate, nitrate, and ammonium), sea salt components, and water-soluble organic carbon, is solely a function of relative humidity (RH) in the algorithm (Li et al., 2021). These simplifications could lead to large discrepancies in polluted regions. For instance, the deviations between observed and estimated b_{ext} values were reported as 15%, 36%, and 37% in Xi'an, Shanghai, and Guangzhou, respectively (Cheng et al., 2015; Cao et al., 2012; Jung et al., 2009). Thus, region-specific adjustments are necessary to reflect the impact of particle compositions on these parameters from site to site.

Many long-term monitoring programs have been implemented to formulate pollution control strategies and explore underlying factors of aerosol properties variation. For example, the IMPROVE program in the United States, initiated in 1985, tracks visibility trends and their driving factors (Epa, 2011). The Southeastern Aerosol Research and Characterization (SEARCH) network, established in 1998, provides detailed insights into aerosol chemistry and precursor gases (Blanchard et al., 2013). In Europe, the European Monitoring and Evaluation Program (EMEP) has operated since 2004 to address air pollution issues related to acidification, eutrophication, and climate impacts (Emep, 2024). In China, long–term $PM_{2.5}$ monitoring began in Hong Kong, where the Environmental Protection Department (HKEPD) initiated comprehensive chemical composition measurements in 1999. Subsequent collaborations expanded the monitoring network to encompass the Guangdong–Hong Kong–Macao Greater Bay Area in 2015 (Hkepd, 2021; Chow et al., 2022).

As one of the most outstanding areas for air pollution improvement, PRD first met National Ambient Air Quality Standards (AQS) for annual average $PM_{2.5}$ (35 μg m^{-3}) in 2015 (Department of Ecology and Environment of Guangdong Province, 2016). $PM_{2.5}$ in the PRD (32.2–46.1 μg m^{-3}) was significantly lower than the YRD (44.8–67.1 μg m^{-3}), the North China Plain (NCP) (64.0–101.9 μg m^{-3}), and other regions (45.1–65.4 μg m^{-3}) (Zhang et al., 2019). Regarding chemical composition, NO_3^- was the dominant species in the YRD and the NCP. However, OM constitutes the largest fraction in the

https://doi.org/10.5194/egusphere-2025-2204
Preprint. Discussion started: 28 May 2025

PRD, similar to other low $PM_{2.5}$ areas worldwide (Geng et al., 2019; Wang et al., 2022b; Yang et al., 2023; Ming et al., 2017; Zhang et al., 2007). So far, long-term studies of $PM_{2.5}$ chemical components in the PRD remain scarce. Fu et al. observed substantial reductions in OC and SO_4^{2-} and stable NO_3^- during 2007–2011, alongside increased aerosol pH and decreased light extinction (2015; 2016; Fu et al., 2014). But this study did not cover the post–2013 period, a key period for air quality improvement. Yan et al. (2020) conducted a meta–analysis (2004−2019), identifying three stages of decline, rise, and stabilization in the fractions of secondary species. Chow et al. (2022) reported the reduction in NO_3^- (66%), EC (60%), hopanes (75%), and K^+ (60%) exceeding that of $PM_{2.5}$ (40%), confirming effective control of vehicular emissions and biomass burning in Hong Kong (2008–2017). These studies observed an unproportional relationships between SO_4^{2-}/SO_2, as well as NO_3^-/NO_2, but the underlying reasons remain unclear. Besides, long-term trends of aerosol acidity, ALWC, and light extinction, which were highly dependent on $PM_{2.5}$ chemical composition, were not fully analyzed. These limitations underscore the need for a more comprehensive, long-term study to explore the underlying mechanisms behind these changes in the PRD.

Our study presents a comprehensive analysis of 532 quartz filter–based $PM_{2.5}$ samples collected over 14 years (2007–2020) at a regional background station. We examined the evolving $PM_{2.5}$ chemical composition, focusing on both primary and secondary species. The unproportional relationships between SO_4^{2-}/SO_2, as well as NO_3^-/NO_2 will be discussed. In addition, we also analyzed variations of aerosol pH, ALWC, and light extinction under the influence of changes in $PM_{2.5}$ chemical composition.

2. Methodology

2.1 Field sampling

The typical Asian monsoon climate influences the PRD region. In summertime, prevailing southwesterly winds bring humid and clean air mass from South China Sea or the northwestern Pacific Ocean. In contrast, during the fall and winter, prevailing northerly winds carry dry and polluted air mass from northern continent. Additionally, the region is often influenced by high–pressure ridges in the fall and winter, which results in a low boundary layer and a high frequency of inversion. These conditions facilitate the accumulation of pollutants. Consequently, $PM_{2.5}$ and other pollutants show a distinct summer–winter contrast, with significantly elevated pollutant levels in fall and winter (Chow et al., 2022; Fu et al., 2014). Our field campaigns were mainly conducted from October to December.

The sampling site, Wanqingsha (WQS; 22.42°N, 113.32°E), is located in a rural area of Guangzhou and the center of the PRD region (Fig. 1). Local anthropogenic emissions have limited influence on this site due to low traffic flow and few factories in the surrounding area. This makes it an ideal background site for investigating regional air pollution. Twenty–four–

https://doi.org/10.5194/egusphere-2025-2204
Preprint. Discussion started: 28 May 2025

hour sampling was conducted using a $PM_{2.5}$ sampler equipped with quartz filters (8 in.×10 in.) at a flow rate of 1.1 m^3 min^{-1}. The quartz filters were pre–baked at 450°C for four hours prior to field sampling and stored at −20°C after sampling until analysis. During the sampling periods, blank samples were collected at monthly intervals. A total of 532 samples were collected and analyzed in this study. Gaseous pollutants data (SO_2, NO_2, NO, and O_3) and meteorological parameters were obtained from an air quality monitoring station operated at WQS. The gaseous pollutant data during 2012–2013 were unavailable because the station was under maintenance.

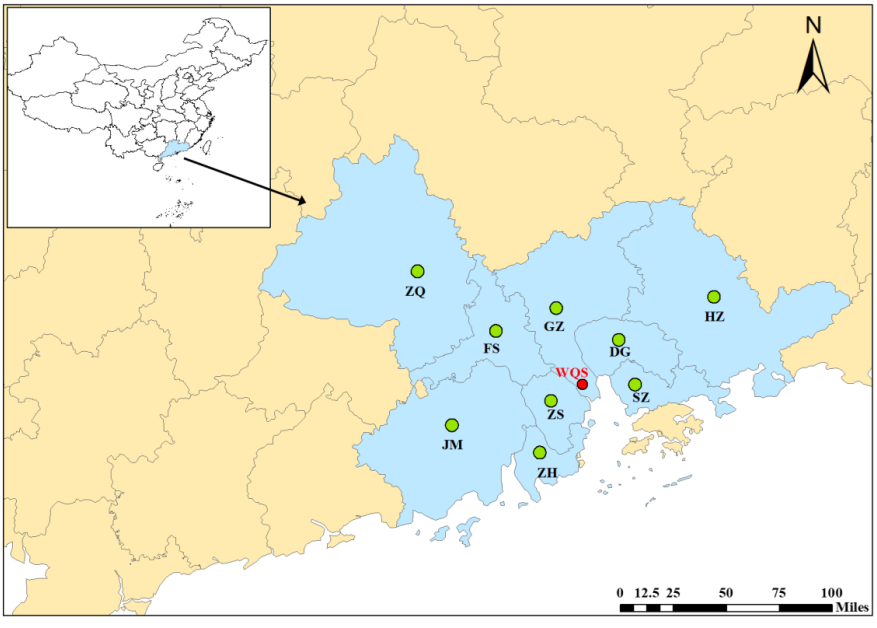

Figure 1. PRD region consists of Guangzhou (GZ), Shenzhen (SZ), Zhuhai (ZH), Dongguan (DG), Foshan (FS), Huizhou (HZ), Zhongshan (ZS), Zhaoqing (ZQ), and Jiangmen (JM). The sampling site WQS is located in the central area of this region.

2.2 Chemical analysis

The organic carbon (OC) and elemental carbon (EC) were determined by the thermo–optical transmittance (TOT) method (NIOSH, 1999) using an OC/EC analyzer (Sunset Laboratory Inc., USA), with a punch (1.5 × 1.0 cm) of the sampled filters. For the water–soluble inorganic ions, a punch (5.06 cm^2) of the filters was extracted twice with 10 ml ultrapure Milli–Q water (18.2 MΩ cm/25 °C) each for 15 min using an ultrasonic ice–water bath. The total water extracts (20 ml) were filtered through a 0.22 μm pore size filter and then stored in a pre–cleaned HDPE bottle. The cations (i.e., Na^+, NH_4^+, K^+, Mg^{2+}, and Ca^{2+}) and anions (i.e., Cl^-, NO_3^-, and SO_4^{2-}) were analyzed with an ion–chromatography system (Metrohm, 883 Basic IC plus). Cations were measured using a Metrohm Metrosep C4–100 column with 2 mmol L^{-1} sulfuric acid as the eluent. Anions were

https://doi.org/10.5194/egusphere-2025-2204
Preprint. Discussion started: 28 May 2025

measured using a Metrohm Metrosep A sup 5–150 column equipped with a suppressor. The anion eluent was a solution of 3.2 mmol L^{-1} Na_2CO_3 and 1.0 mmol L^{-1} $NaHCO_3$.

2.3 Quality assurance/quality control (QA/QC)

Field and laboratory blank samples were analyzed in the same way as field samples. All the OC/EC and cation/anion data were corrected using the field blanks. The method detection limits (MDLs) were 0.01–0.05 μg m^{-3} for the OC, EC, cations, and anions. Ion balance was employed as a quality control check in the anion/cation analysis. A significant linear correlation (R^2 = 0.97) was observed between anions and cations, with a slope of 0.82 for all $PM_{2.5}$ samples. This slope, being close to unity, indicated that all the significant ions were resolved. Before data analyze, all data were manually inspected and outliers (i.e., $X_{75\%}+3(X_{75\%}-X_{25\%})$) were removed to rule out the influence of extreme concentrations on overall trends.

2.4 Estimation of primary organic carbon (POC) and secondary organic carbon (SOC)

EC is a product of carbon fuel–based combustion processes and is exclusively associated with primary emissions, whereas OC can be from both direct emissions and be formed through secondary pathways. Differentiation between primary organic carbon (POC) and secondary organic carbon (SOC) is indispensable for probing atmospheric aging processes of organic aerosols. EC–tracer method was widely used to estimate POC and SOC (Turpin and Huntzicker, 1991; 1995). However, a previous study revealed that EC–tracer method would return higher estimation of SOC (Kim et al., 2012). Recently, Liao et al. (2023) proposed Bayesian Inference Approach and suggested it had significant advantages in accurately estimating POC and SOC compared to the conventional method, such as EC–tracer method, minimum ratio value, minimum R squared, and multiple linear regression. In this study, we used Bayesian Inference Approach which has the convenience of relying only on the commonly available mass concentrations of EC and SO_4^{2-} to estimate POC and SOC. They can be calculated as following:

$$SOC = K_{EC} \times [EC] + K_{SO42-} \times [SO_4^{2-}] \quad (1)$$

$$POC = OC - SOC \quad (2)$$

Where K_{EC} and K_{SO42-} are parameters calculated by Bayesian Inference Approach in R language, the details can be found in previous research (Liao et al., 2023). The variations of K value are shown in Fig. S1. Given intense photochemical reactions and larger fractions of aged aerosols in the PRD, a higher conversion factor of 2.4 was employed to convert SOC to SOA (Yan et al., 2020).

https://doi.org/10.5194/egusphere-2025-2204
Preprint. Discussion started: 28 May 2025

3. Results and discussion

3.1 Long–term trends of $PM_{2.5}$ and its chemical composition

In response to severe particle pollution, the Chinese government issued the Air Pollution Prevention and Control Action Plan in 2013. Due to the strengthened emission controls in the PRD, primary pollutants have been reduced significantly over the past decades (Bian et al., 2019). Based on daily $PM_{2.5}$ concentrations in our samples, we divided the data into five groups according to interim targets recommended by the Worle Health Organization (WHO) in 2021 (World Health Organization, 2021): IT0 ($PM_{2.5}$ > 75 μg m^{-3}), IT1 (75 μg m^{-3} > $PM_{2.5}$ > 50 μg m^{-3}), IT2 (50 μg m^{-3} > $PM_{2.5}$ > 37.5 μg m^{-3}), IT3 (37.5 μg m^{-3} > $PM_{2.5}$ > 25 μg m^{-3}), and IT4 (25 μg m^{-3} > $PM_{2.5}$). The majority of samples fell into T0 and T1 categories (41%–100%) before 2013, while this ratio quickly decreased (8%–60%) during 2013–2020 (Fig. S2), indicating successful implementation of air pollution mitigation strategies after 2013.

Annual average concentrations of $PM_{2.5}$ and its chemical composition are presented in Fig. 2a. From 2007 to 2020, $PM_{2.5}$ concentrations exhibited a significant decline from 87.1 ± 15.5 μg m^{-3} to 34.0 ± 11.3 μg m^{-3}, at a rate of –4.0 μg m^{-3} yr^{-1} (p < 0.01). This trend aligns with the previous results from meta–analysis (–3.9 μg m^{-3} yr^{-1}) and regional simulation (–4.0 μg m^{-3} yr^{-1}) in the PRD (Yan et al., 2020; Zhang et al., 2019), affirming WQS can serve as a regional background site. During this period of air quality improvement, OM (defined as OC × 1.6) (Yang et al., 2023) remained the most abundant component (25%–47%) in $PM_{2.5}$, followed by SO_4^{2-} (16%–26%), NO_3^- (7%–18%), NH_4^+ (7%–10%) and EC (3%–8%). Other ions, such as Cl^-, Na^+, K^+, Mg^{2+}, and Ca^{2+}, contributed less than 3% each to the mass of $PM_{2.5}$. In China, desulfurization regulation for power plants was enforced around 2005, resulting in a notable decline (–7%) in the proportion of SO_4^{2-} (Fig. 2b-c). However, the installation of denitrification devices on power plants began in late 2011 and started to take effect in 2012. With the delayed implementation of NO_x emissions control measures compared to those for SO_2 (Fu et al., 2014; Geng et al., 2017; Qu et al., 2017; Reuter et al., 2014), the mass fractions of NO_3^- increased by 10%. By the end of 2020, the proportion of NO_3^- had doubled compared to 2007, approaching the level of SO_4^{2-}. The proportion of OM also increased from 36% to 43%. Consequently, future air pollution control efforts need to focus on reducing OM and NO_3^- concentrations to continue improving air quality in the PRD region.

https://doi.org/10.5194/egusphere-2025-2204
Preprint. Discussion started: 28 May 2025

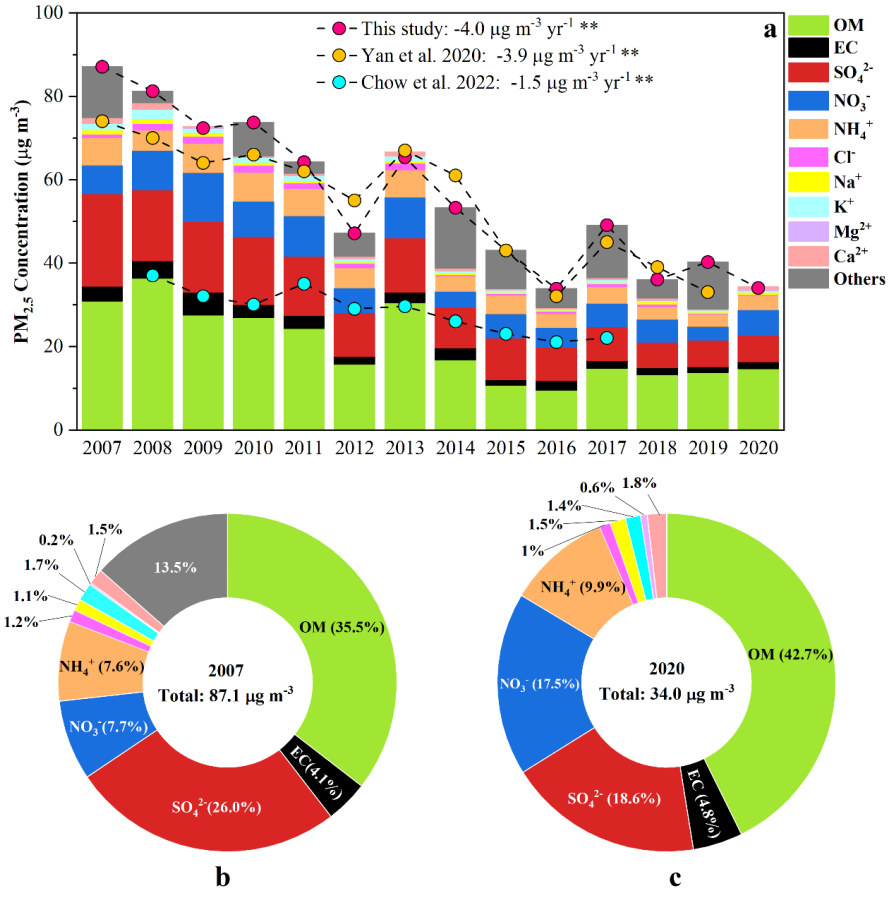

Figure 2. (a) Trends of $PM_{2.5}$ and its major components. Bars represent concentrations of chemical compositions and circles represent concentrations of $PM_{2.5}$ in different studies. (b), (c) The comparison of the mass fractions of major components in 2007 and 2022.

The chemical composition of $PM_{2.5}$ can be categorized into primary species and secondary species. Primary species consist of POA, EC, metal ions (e.g., Cl^-, Na^+, K^+, Mg^{2+}, Ca^{2+} etc.). Secondary species include SOA and SIA (SO_4^{2-}, NO_3^-, and NH_4^+). Our results indicated that secondary species consistently dominated over primary species in $PM_{2.5}$ composition, accounting for 54% to 79% of the total mass (Fig. 3a). Additionally, secondary species declined at a faster rate (–2.45 μg m^{-3} yr^{-1}, $p < 0.01$) compared to primary species (–1.48 μg m^{-3} yr^{-1}, $p < 0.01$), indicating reduction of secondary species had more contribution in particulate pollution mitigation. Although Yan et al. (2020) also observed a decline trend in concentrations of secondary species after 2008 in the PRD, the proportion of secondary species was stable around 80%, which was higher than our study. This might stem from the fact that the EC–tracer method applied by the previous study would return higher estimation of SOC, which made secondary species increase (Kim et al., 2012). Our result suggested that the average

https://doi.org/10.5194/egusphere-2025-2204
Preprint. Discussion started: 28 May 2025

concentration of SOC estimated by the Bayesian Inference Approach was ~30% lower than that by the EC–tracer method and more reliable (Fig. S3). We calculated K values on an annual basis to further estimate SOC, whereas Yan et al. used a fixed value of $(OC/EC)_{pri}$ (the minimum value of all collected data) to estimate SOC. As a result, the proportion of secondary species in this study showed greater variability than that of Yan et al. Additionally, we analyzed the proportion of secondary species under different pollution levels. Fig. 3b showed that the mass fraction of secondary species increased significantly from 57% to 73% with the improvement of air quality (from IT0 to IT4). This meant secondary species play an increasingly prominent role in lower $PM_{2.5}$ levels.

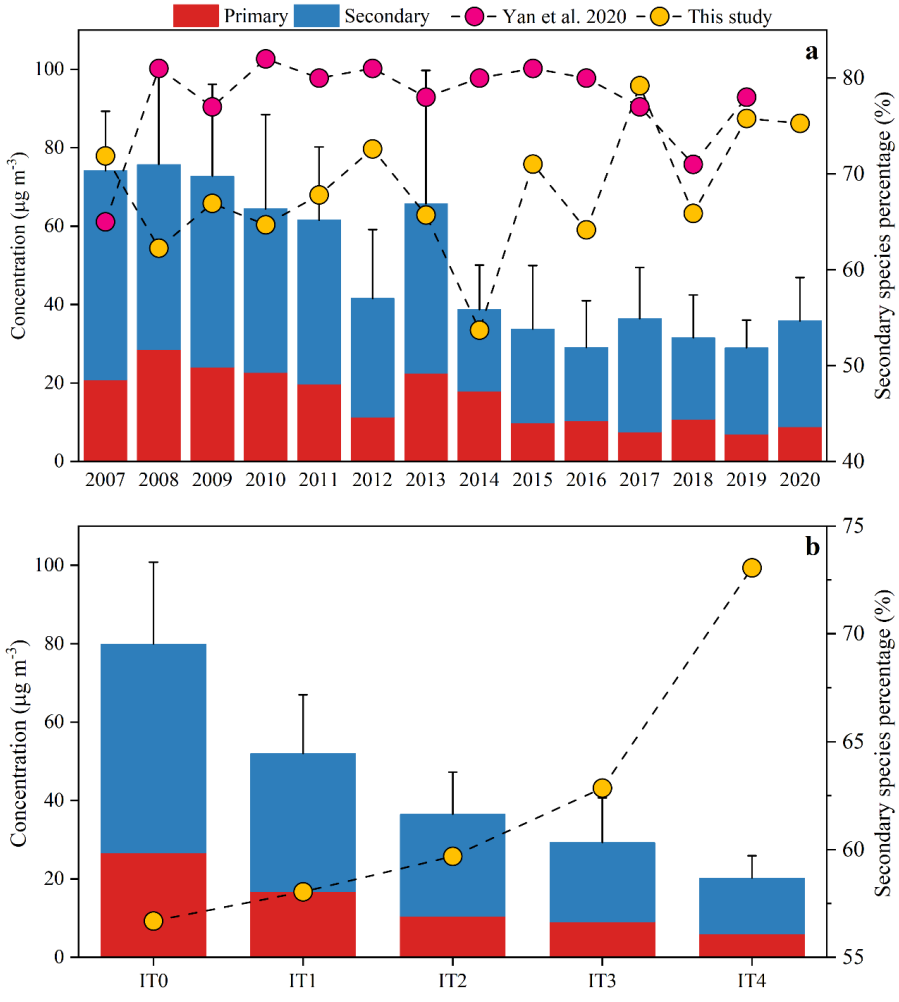

Figure 3. Primary and secondary species variations during 2007–2020 (a) and their variations under different pollutants levels (b). Bars represent concentrations of them and circles represent the mass proportion of secondary species in $PM_{2.5}$. Secondary species (accounts for 54%–79%) dominated over primary species. The proportion of secondary species increased from 57% to 73% with improvement of air quality (From IT0 to IT4).

https://doi.org/10.5194/egusphere-2025-2204
Preprint. Discussion started: 28 May 2025

3.2 Annual variations of primary species and secondary species

3.2.1 Primary species

The trends of individual components in $PM_{2.5}$ can be seen in Fig. S4–5. POA exhibited the most significant decline at a rate of –0.97 μg m^{-3} yr^{-1} (–9% yr^{-1}, $p < 0.01$). EC serves as a tracer for primary combustion, K^+ serves as a tracer for biomass burning, and Ca^{2+} could be applied to track dust-related sources (Turpin and Huntzicker, 1991; Zhu et al., 2017). Despite the slight decline in their concentrations, our result showed that the relative reductions of EC (–9% yr^{-1}), K^+ (–12%) and Ca^{2+} (–11% yr^{-1}) were greater than that of $PM_{2.5}$ (–7% yr^{-1}), confirming that control measures for these sources had been effective. Cl^- and Na^+ also showed decline trends at rates of –0.10 μg m^{-3} yr^{-1} (–10% yr^{-1}), –0.05 μg m^{-3} yr^{-1} (–9% yr^{-1}), respectively ($p < 0.01$). Marine emission is considered the biggest source of Cl^- in fine particle. However, anthropogenic sources such as coal combustion and biomass burning also had non–negligible impacts on it (Luo et al., 2019). After excluding the influence of anthropogenic sources (Text S1 and Fig. S6), Cl^- showed only a slight decline (–2% yr^{-1}), suggesting that the contribution from marine emissions to $PM_{2.5}$ remained largely stable.

3.2.2 Secondary species

SO_4^{2-} showed a clear decrease at –1.13 μg m^{-3} yr^{-1} (–10% yr^{-1}, $p < 0.01$), whereas NO_3^- and NH_4^+ showed moderate declines (–0.40 μg m^{-3} yr^{-1}, –6% yr^{-1}; –0.31 μg m^{-3} yr^{-1}, –6% yr^{-1}, respectively, $p < 0.05$). Strong correlations between SO_4^{2-}/SO_2, as well as between NO_3^-/NO_2 were observed (Fig. S7), suggesting that reductions of SO_4^{2-} and NO_3^- were mainly driven by reductions of their gaseous precursors. With relative humidity (RH) rising, the slopes of SO_4^{2-}/SO_2, as well as NO_3^-/NO_2, increased, indicating enhanced conversion of primary pollutants to secondary species. The generally lower intercepts observed in the NO_3^-/NO_2 regression compared to those in the SO_4^{2-}/SO_2 regression could be explained by the semi-volatile nature of nitrate. When NO_2 levels are low, the accumulation of nitrate is hindered due to volatilization losses. In contrast, sulfate is the least volatile among all the inorganic aerosol components (Kang et al., 2022), allowing it to persist even at low SO_2 concentrations. Notably, SO_4^{2-} reduction (–10% yr^{-1}) lagged behind SO_2 reduction (–13% yr^{-1}), while NO_3^- reduction (–6% yr^{-1}) outpaced that of NO_2 (–3% yr^{-1}) (Fig. 4). Other studies have also observed these disproportionate changes, but the reasons behind remained unclear (Chow et al., 2022; Yan et al., 2020; Geng et al., 2019; Blanchard et al., 2013).

https://doi.org/10.5194/egusphere-2025-2204
Preprint. Discussion started: 28 May 2025

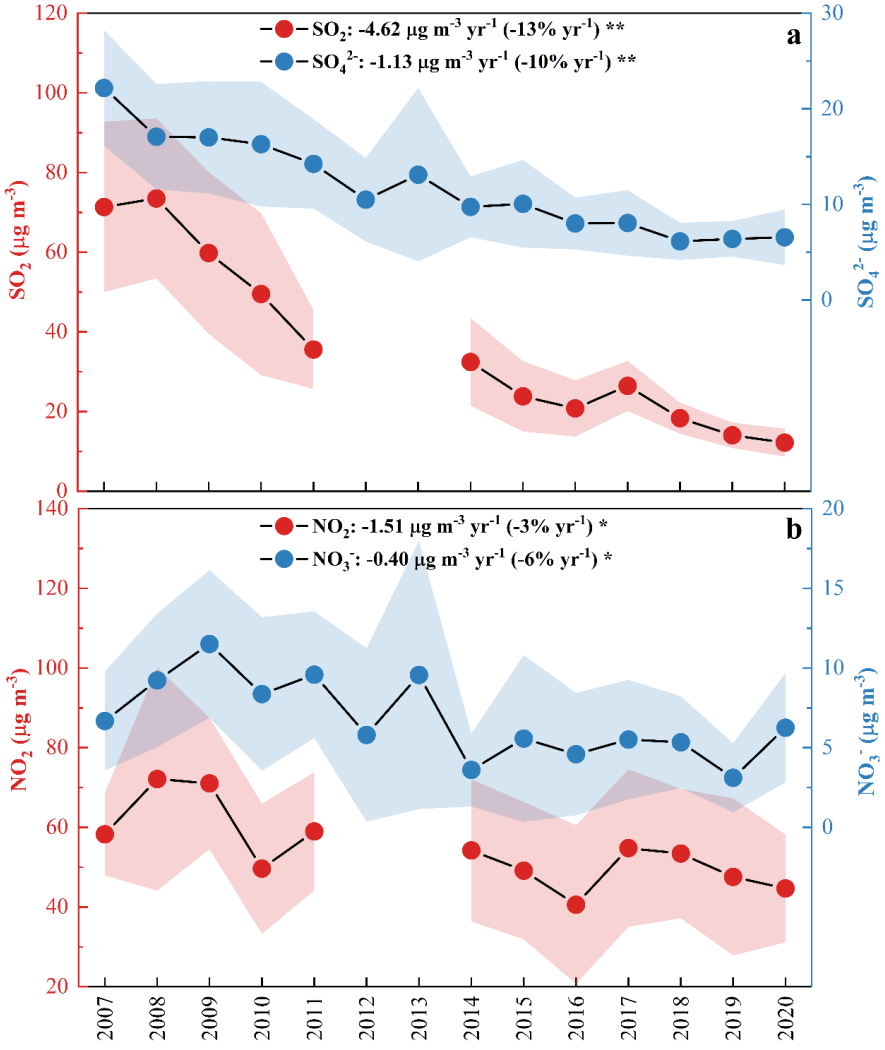

250 **Figure 4. (a) Annual variations of SO_4^{2-} and SO_2. (b) Annual variations of NO_3^- and NO_2. The shaded region indicates the uncertainty bounds. One asterisk, two asterisks denote *p* value < 0.05, 0.01, respectively. In the PRD, SO_4^{2-} and SO_2 showed a more significant decline than NO_3^- and NO_2. The reduction of SO_4^{2-} (–10% yr^{-1}) was slower than SO_2 (–13% yr^{-1}), while reduction of NO_3^- (–6% yr^{-1}) was faster than NO_2 (–3% yr^{-1}).**

255 Here, we calculated SOR and NOR (Li et al., 2023) described in equations (3–4), where *n* refers to the molar concentration. The higher SOR and NOR represent more efficient conversion of gaseous species into secondary aerosols.

$$SOR = \frac{n[SO_4^{2-}]}{n[SO_4^{2-}] + n[SO_2]} \quad (3)$$

$$NOR = \frac{n[NO_3^-]}{n[NO_3^-] + n[NO_2]} \quad (4)$$

https://doi.org/10.5194/egusphere-2025-2204
Preprint. Discussion started: 28 May 2025

As shown in Fig 5a, a dramatic increase in SOR was observed during 2007–2020 ($p < 0.05$). The SOR value in 2020 (0.24 ± 0.09) was twice as high as that in 2008 (0.12 ± 0.07). The more efficient SO_4^{2-} formation from SO_2 oxidation slowed down the reduction of SO_4^{2-} alongside decreasing SO_2 levels. Gas–phase oxidation of SO_2 followed by neutralization and aerosol phase condensation, is an important SO_4^{2-} formation pathway (Berndt et al., 2023). Heterogeneous processes, including SO_2 transfer to the aerosol phase, dissolution, and oxidation by oxidants such as H_2O_2 and O_3, also contribute significantly in polluted regions (Wang et al., 2016; Liu et al., 2021). The solubility and effective Henry's law constant of SO_2 are positively pH-dependent (Seinfeld et al., 1998). Higher pH promotes the dissolution of SO_2 in water, which will enhance SO_4^{2-} formation. ALWC plays a key role in determining the aqueous oxidation rate and mass transfer. In addition, high temperature can facilitate both gas–phase and aqueous–phase reactions. As shown in Fig. S8, there were strong positive correlations between SOR and O_3 (r = 0.45), temperature (r = 0.48), as well as ALWC (r = 0.23). But there was no significant correlation between SOR and pH. A possible explanation is that hydrogen ions facilitate aqueous-phase oxidation of SO_2 by H_2O_2, which will offset the effect of reduced SO_2 solubility under low pH conditions (Liu et al., 2021). To assess the impacts of these factors on SOR and eliminate dimensional and order of magnitude effects, a normalized multiple linear regression was developed as below:

$$SOR = 0.025 \times O_3 + 0.017 \times ALWC + 0.019 \times Temperature + 0.190 \quad (5)$$

The prediction of SOR showed good agreement with the observations (Fig. S9a). The larger regression coefficients of O_3 and temperature, along with their stronger correlations with SOR, suggested that the increase of SOR was mainly driven by the two factors. Our result showed that ALWC exhibited a downward trend (Fig. 6b), which exerted a negative influence on SOR. Although O_3 concentration did not show an obvious trend at our measurement station (Fig. S10a), a previous study suggested that there was a rapid increase of O_3 in the PRD after 2013 (Cao et al., 2024). Meanwhile, the temperature also rose slightly ($p < 0.05$) during the past decade (Fig. S10b). Consequently, a significant upward trend was observed in SOR.

NOR did not show a clear trend, but the average values before 2013 (NOR > 0.07) were higher than those in later years (NOR < 0.07) (Fig. 5b, t–test, $p < 0.01$). This meant that conversion of NO_2 into NO_3^- became weaker, resulting in a greater reduction in NO_3^- compared to NO_2. NO_3^- can be formed during both daytime and nighttime. During the day, HNO_3 is produced via the gas–phase reaction between OH and NO_2 and then neutralized by NH_3 to produce NO_3^- (R1–R2) (Calvert and Stockwell, 1983). During nighttime, NO_2 can also be oxidized by O_3 to generate NO_3 which further reacts with NO_2 to produce N_2O_5. Heterogeneous uptake of N_2O_5 is a vital nitrate formation pathway during nighttime (R3–R5) (Finlayson-Pitts et al., 1989). Fig. S11 showed that there were positive correlations between NOR and O_3 (r = 0.12), pH (r = 0.25), as well as ALWC (r = 0.55). Different from SOR, higher temperature prevents N_2O_5 formation and promotes evaporation of HNO_3 from particle–phase to gas–phase, resulting a negative correlation between NOR and temperature (r = –0.18). The result of normalized multiple linear regression for NOR is as below:

https://doi.org/10.5194/egusphere-2025-2204
Preprint. Discussion started: 28 May 2025

$$NOR = 0.012 \times O_3 + 0.025 \times ALWC - 0.011 \times Temperature + 0.008 \times pH + 0.081 \quad (6)$$

The prediction of NOR showed good agreement with the observations (Fig. S9b). The largest regression coefficient and the strongest correlation between ALWC and NOR suggested that NOR was more sensitive to the changes in ALWC. Lower ALWC after 2013 (Fig. 6b) did not favor heterogeneous nitrate formation, this overall lower NOR led to larger reduction in NO_3^- compared to NO_2.

$$OH\ (g) + NO_2\ (g) + M \rightarrow HNO_3\ (g) + M \quad (R1)$$

$$HNO_3(g) + NH_3\ (g) \leftrightarrow NO_3^-(aq) + NH_4^+(aq) \quad (R2)$$

$$NO_2\ (g) + O_3\ (g) \rightarrow NO_3\ (g) \quad (R3)$$

$$NO_2\ (g) + NO_3\ (g) + M \leftrightarrow N_2O_5\ (g) + M \quad (R4)$$

$$N_2O_5\ (g) + H_2O\ (aq) + Cl^-(aq) \leftrightarrow (2-\emptyset)NO_3^-(aq) + \emptyset ClNO_2 \quad (R5)$$

The gas-particle conversion of NH_3 could be affected by anions in particle–phase. Due to the decrease of $2 \times n(SO_4^{2-}) + n(NO_3^-)$ (Fig. S12), less NH_3 was needed to neutralize H_2SO_4 and HNO_3. This resulted in a slight decline in NH_4^+ (–0.31 μg m^{-3} yr^{-1}, $p < 0.01$), while NH_3 emissions remained steady (Geng et al., 2019).

SOA is formed through the oxidation of VOCs, followed by gas–particle partitioning. Although VOCs emission kept rising (Bian et al., 2019; Guo et al., 2024) and concentration of O_3 fluctuated (Fig. S10a) during the past decade, SOA declined significantly (–0.74 μg m^{-3} yr^{-1}, $p < 0.01$). This could result from the reductions in aerosol acidity and ALWC (which will be discussed in Sect. 3.3). As SOA accounted for more than 50% of OM, more efforts are needed to reduce it.

https://doi.org/10.5194/egusphere-2025-2204
Preprint. Discussion started: 28 May 2025

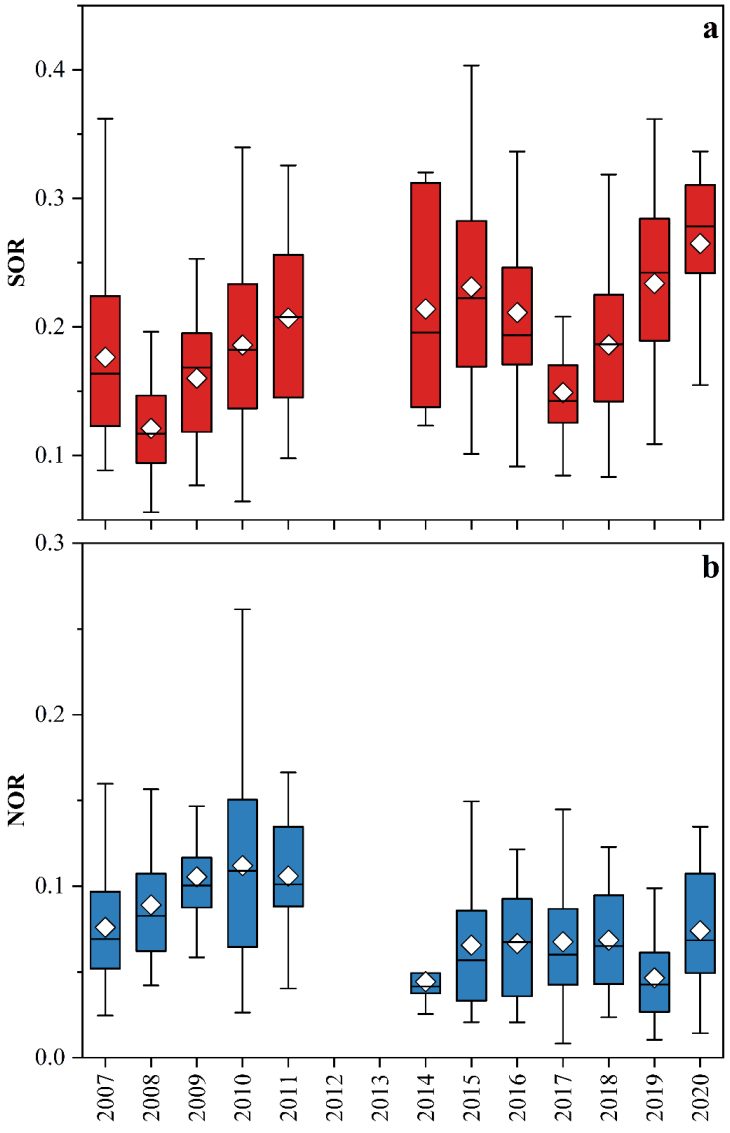

Figure 5. The variations of SOR (a) and NOR (b). A dramatic increase in SOR was observed ($p < 0.05$) and the SOR value in 2020 (0.24 ± 0.09) was twice as high as that in 2008 (0.12 ± 0.07). Although there was no significant trend in NOR, the value before 2012 was higher than that after 2013.

310

https://doi.org/10.5194/egusphere-2025-2204
Preprint. Discussion started: 28 May 2025

3.3 Impact of changes of major components on aerosol pH and ALWC

ISORROPIA II, a thermodynamic equilibrium model for the $K^+ – Ca^{2+} – Mg^{2+} – NH_4^+ – Na^+ – SO_4^{2-} – NO_3^- – Cl^- – H_2O$ aerosol system (Fountoukis and Nenes, 2007), has been widely applied to estimate aerosol pH and ALWC. Here, we applied ISORROPIA–II to estimate aerosol pH and ALWC from 2007 to 2020. Due to the unavailability of gas–phase concentrations of HNO_3, HCl, and NH_3 during our campaign period, we conducted four iterations to produce the result optimally (Text S2, Fig. S13–14). The annual variations of pH and ALWC are shown in Fig. 6. As discussed earlier, the reductions in acidic components (SO_4^{2-} and NO_3^-) were greater than that in the alkaline component (NH_4^+), leading to a significant decrease in acidity. Aerosol pH increased from 1.51 ± 1.07 to 3.29 ± 1.43, at a rate of 0.06 yr^{-1} ($p < 0.05$). A sharp increase of aerosol pH occurred during 2007–2012 due to rapid decline of SO_4^{2-} during this period. As Fu et al. (2015) did not include the gas–phase data in pH calculation, the pH values reported by them (-1.11–0.81) were significantly lower than those in this study (1.51–2.60) during the same period. Our results showed that ALWC decreased from 20.5 ± 10.0 to 8.7 ± 4.5 μg m^{-3}, at a rate of –1.1 μg m^{-3} yr^{-1} ($p < 0.01$). Unexpectedly, low ALWC was observed in 2008 when SIA concentrations, which enhance the hygroscopicity of particulate matter, were at very high levels. It might be associated with low RH (Table S1). To eliminate the influence of changes in meteorological conditions, we used annual average temperature and RH during the entire campaign period as input to recalculate pH and ALWC. The results showed a clear enhancement of ALWC in 2008 (Fig. S15), and the upward trend in pH and downward trend in ALWC still persisted. This demonstrated the long–term trends of pH and ALWC were mainly driven by the changes in chemical composition of $PM_{2.5}$. As we discussed in Sect. 3.2.2, ALWC exhibited positive correlations with SOR and NOR. This indicated a positive feedback mechanism in which the reductions in hygroscopic components (e.g., sulfate and nitrate) leaded to lower ALWC, thereby suppressing SIA formation. Recent studies demonstrated that high aerosol acidity, ALWC, and O_3 facilitated SOA formation (Zhang et al., 2024; Zhang et al., 2022b; Ma et al., 2024). Our results also showed that SOA was positively correlated with ALWC and O_3, but negatively correlated with pH (Fig. S16). In this study, SOA declined significantly (Fig. S5) while the emission of VOCs (Bian et al., 2019; Guo et al., 2024) and O_3 (Cao et al., 2024) kept rising in the PRD. Consequently, the trend of SOA was mainly driven by the reductions in aerosol acidity and ALWC.

https://doi.org/10.5194/egusphere-2025-2204
Preprint. Discussion started: 28 May 2025

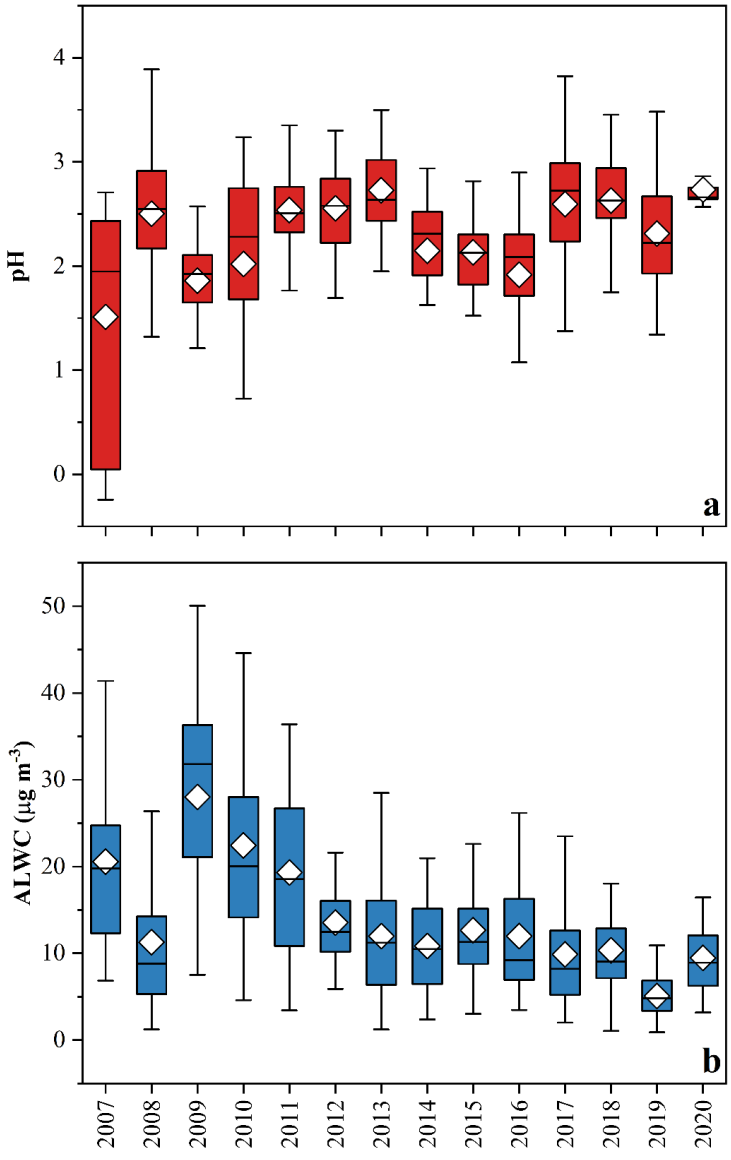

Figure 6. (a) Annual average pH increased at a rate of 0.06 yr^{-1}. (b) Annual average ALWC decreased at a rate of –1.1 μg m^{-3} yr^{-1}.

We further investigated changes in pH and ALWC under different pollution levels. As Fig. S17 presented, low pH occurred under elevated pollutant level (IT0), while pH values were close under other levels (IT1–IT4). Additionally, there was no significant difference between the recalculated pH (eliminating the influence of meteorological factors) and the original one, indicating limited impacts of variations of temperature and RH on aerosol acidity. ALWC showed a clear decline pattern with decreasing pollutant levels (IT0–IT4). A significant difference (18%–35%, $p < 0.01$) was observed between the

https://doi.org/10.5194/egusphere-2025-2204
Preprint. Discussion started: 28 May 2025

recalculation and original results under IT2–IT4, indicating temperature and RH also exerted a significant influence on ALWC under lower pollution levels.

3.4 Impact of changes of major components on extinction coefficient

We adopted MSE/MAE suggested by Fu et al. (2016) and relationship between chemical composition and f(RH) suggested by Li et al. (2021) to reconstruct b_{ext} using equations (5-8). [*AS*], [*AN*], [*SS*], [*LAC*] refer to mass concentrations (μg m^{-3}) of NH_4SO_4, NH_4NO_3, sea salt, and EC, respectively. The details of $PM_{2.5}$ reconstruction method followed the previous study (Chow et al., 2015), i.e., $AS = 1.375 \times SO_4^{2-}$, $AN = 1.29 \times NO_3^-$, $LAC = EC$ and $SS = 1.8 \times Cl^-$. RH_{ref} was threshold of high RH, 40% was used here.

$$b_{ext} = 6.5 \times [OM] + 2.6 \times f(\mathrm{RH}) \times [AS] + 2.4 \times f(\mathrm{RH}) \times [AN] + 7.3 \times f(\mathrm{RH})_{ss} \times [SS] + 7.7 \times [LAC] \quad (5)$$

$$f(\mathrm{RH}) = [\,(1-RH)/(1-\mathrm{RH}_{ref})\,]^{-\gamma} \quad (6)$$

$$\gamma = 0.48 \times F + 0.59 \quad (7)$$

$$F = (OC+EC)/(OC+EC+SO_4^{2-}+NO_3^-+NH_4^+) \quad (8)$$

Our results showed that b_{ext} in the PRD decreased significantly at a rate of -21.44 Mm^{-1} yr^{-1} ($p < 0.01$), aligning with the overall decline of $PM_{2.5}$ (Fig. 7). However, the highest b_{ext} was unexpectedly observed in 2009, even though $PM_{2.5}$ concentration was lower than 2007 and 2008. This anomaly could result from the highest RH in 2009. As illustrated in Fig. S18, OM dominated b_{ext} (44%–61%), followed by $(NH_4)_2SO_4$ (15%–28%) and NH_4NO_3 (6%–13%). The proportion of SIA (F) fluctuated during 2007–2020, which leaded to a change in f(RH) and then further influenced b_{ext}. As a result, we found that the chemical budget of b_{ext} from $(NH_4)_2SO_4$ did not exhibit a continuous decline trend, while the mass concentration and proportion of SO_4^{2-} in $PM_{2.5}$ decreased significantly.

We also calculated b_{ext} by IMPROVE formula and compared to the local parameter scheme (Fig. S19). Generally, b_{ext} estimated by IMPROVE formula (335.72 ± 219.64 Mm^{-1}) was significantly higher than that estimated by local parameter scheme (262.67 ± 143.82 Mm^{-1}). We further investigated this discrepancy under different pollution levels. With the improvement in air quality, the difference between the two schemes narrowed gradually ($p < 0.01$). Our results indicated that the IMPROVE equation tend to overestimate b_{ext} in elevated pollution periods. Thus, more site–specific parameters and local parameter scheme are needed in those areas to predict b_{ext} more accurately.

https://doi.org/10.5194/egusphere-2025-2204
Preprint. Discussion started: 28 May 2025

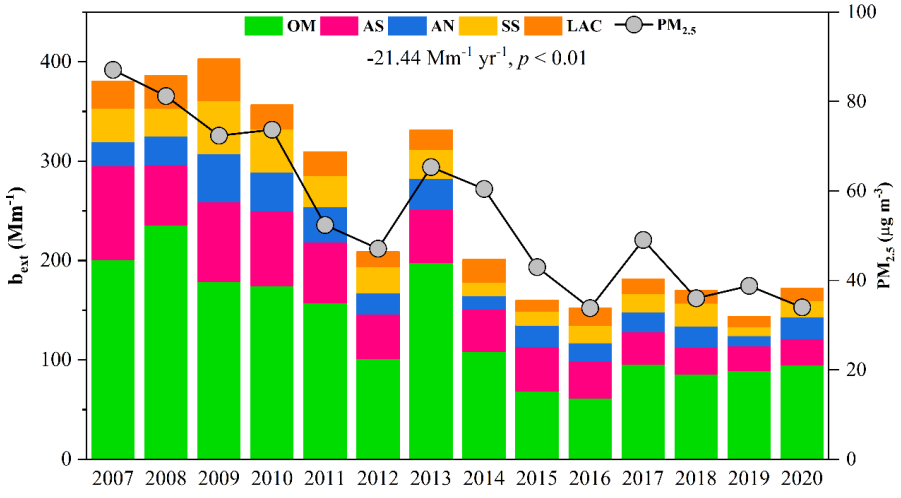

Figure 7. Light extinction coefficient (b_{ext}) in WQS during 2007–2020. It declined at a rate of $-21.44\ Mm^{-1}\ yr^{-1}$ significantly ($p < 0.01$) and its trend aligned with that of $PM_{2.5}$.

4. Conclusions

In this study, we conducted field measurements of $PM_{2.5}$ mass concentrations and its chemical composition at the PRD regional background site during 2007–2020. $PM_{2.5}$ levels showed a significant decline from 87.1 ± 15.5 μg m^{-3} to 34.0 ± 11.3 μg m^{-3} at a rate of –4.0 μg m^{-3} yr^{-1}. Secondary species (54%–79%) dominated over primary species, although the proportion was lower than that reported in a previous study (~80%) in the PRD. This discrepancy could be attributed to an overestimation of SOC caused by the EC-tracer method employed in the previous study. In addition, the mass fraction of secondary species increased with the improvement in air quality, suggesting greater attention should be given to them under cleaner conditions. Among primary species, POA, EC, K^+ and Ca^{2+} exhibited significant declines. This indicated that control measures for combustion emissions, biomass burning and dust-related sources were effective. SIA displayed rapid downward trends among secondary species, particularly for SO_4^{2-}. Due to the delayed control of NO_x emissions compared to SO_2, mass fractions of SO_4^{2-} decreased from 26.0% to 18.6% while NO_3^- increased from 7.7% to 17.5%. By the end of 2020, the proportion of NO_3^- had doubled compared to 2007, approaching the level of SO_4^{2-}. Although many previous studies have observed the disproportionate changes in SO_4^{2-}/SO_2 and NO_3^-/NO_2, underlying causes remained unclear. In this study, we found the disproportionate reductions in SO_4^{2-} (–10% yr^{-1}) compared to SO_2 (–13% yr^{-1}), and in NO_3^- (–6% yr^{-1}) compared to NO_2 (–3% yr^{-1}), which were attributed to an increase in SOR and a decrease in NOR, respectively. Correlation analysis indicated that SOR was primarily influenced by O_3 and temperature, whereas NOR was driven by ALWC.

https://doi.org/10.5194/egusphere-2025-2204
Preprint. Discussion started: 28 May 2025

Aerosol pH and ALWC were estimated using ISORROAPIA–II. Due to the unavailability of gas–phase concentrations of HNO_3, HCl, and NH_3 during our campaign period, we propose a reliable approach involving four iterative calculations to obtain optimal results. Our results showed that aerosol pH increased from 1.51 ± 1.07 to 3.29 ± 1.43 at a rate of 0.06 yr^{-1}. Consistent with previous studies, we found that the impacts of meteorological factors on aerosol pH were limited, while the changes in $PM_{2.5}$ components significantly influence aerosol pH. ALWC decreased significantly at a rate of –1.1 μg m^{-3} yr^{-1} and showed a clear decline pattern with decreasing pollutant levels. This might indicate presence of a positive feedback mechanism between ALWC and hygroscopic components. Given the critical roles of acidity and ALWC in the formation of secondary species, the reductions in acidity and ALWC caused by changes in $PM_{2.5}$ major components may also suppress the formation of SOA in the atmosphere.

In addition, air visibility greatly improved with decline of $PM_{2.5}$ chemical components. We used a local parameter scheme to calculate b_{ext} and demonstrated that it decreased at a rate of –21.44 Mm^{-1} yr^{-1}. The IMRPOVE formula, which employs the fixed f(RH), may lead to overestimation of b_{ext} under high pollution conditions. Thus, more site–specific parameters and local parameter scheme are needed in those areas to predict b_{ext} more accurately.

This study highlights that the changes in $PM_{2.5}$ chemical composition can significantly affect key aerosol physicochemical properties, such as aerosol pH, ALWC, and light extinction coefficient. The variations of aerosol pH and ALWC can, in turn, influence the formation of secondary species. Since the importance of secondary species will become more prominent with continuous air quality improvement, more efforts should focus on them in the future.

Code and data availability. The experimental data in this study are available upon request to the corresponding author by email.

Author contributions. XD conceived the project and designed the study. Y-FH performed the data analysis and wrote the paper. Y-QZ, D-HC, TZ, KY, J-QW, QC, and HJ arranged the sample collection and assisted with the data analysis. Z-RW and PL analyzed the samples. XD, Q-FH, X-MW, and MB performed the data interpretation and edited the paper. All authors contributed to the development of the final paper.

Competing interests. At least one of the (co-)authors is a member of the editorial board of Atmospheric Chemistry and Physics.

Financial support. This research was funded by the National Natural Science Foundation of China (42321003/42177090), Guangdong Foundation for Program of Science and Technology Research (2023B0303000007/2023B1212060049/2024A1515011181).

https://doi.org/10.5194/egusphere-2025-2204
Preprint. Discussion started: 28 May 2025

References

Berndt, T., Hoffmann, E. H., Tilgner, A., Stratmann, F., and Herrmann, H.: Direct sulfuric acid formation from the gas-phase oxidation of reduced-sulfur compounds, Nat. Commun., 14, 4849, https://doi.org/10.1038/s41467-023-40586-2, 2023.

Bian, Y. H., Huang, Z. J., Ou, J. M., Zhong, Z. M., Xu, Y. Q., Zhang, Z. W., Xiao, X., Ye, X., Wu, Y. Q., Yin, X. H., Li, C., Chen, L. F., Shao, M., and Zheng, J. Y.: Evolution of anthropogenic air pollutant emissions in Guangdong Province, China, from 2006 to 2015, Atmos. Chem. Phys., 19, 11701-11719, https://doi.org/10.5194/acp-19-11701-2019, 2019.

Blanchard, C. L., Hidy, G. M., Tanenbaum, S., Edgerton, E. S., and Hartsell, B. E.: The Southeastern Aerosol Research and Characterization (SEARCH) study: Temporal trends in gas and PM concentrations and composition, 1999-2010, Journal of the Air & Waste Management Association, 63, 247-259, https://doi.org/10.1080/10962247.2012.748523, 2013.

Burnett, R., Chen, H., Szyszkowicz, M., Fann, N., Hubbell, B., Pope, C. A., Apte, J. S., Brauer, M., Cohen, A., Weichenthal, S., Coggins, J., Di, Q., Brunekreef, B., Frostad, J., Lim, S. S., Kan, H. D., Walker, K. D., Thurston, G. D., Hayes, R. B., Lim, C. C., Turner, M. C., Jerrett, M., Krewski, D., Gapstur, S. M., Diver, W. R., Ostro, B., Goldberg, D., Crouse, D. L., Martin, R. V., Peters, P., Pinault, L., Tjepkema, M., Donkelaar, A., Villeneuve, P. J., Miller, A. B., Yin, P., Zhou, M. G., Wang, L. J., Janssen, N. A. H., Marra, M., Atkinson, R. W., Tsang, H., Thach, Q., Cannon, J. B., Allen, R. T., Hart, J. E., Laden, F., Cesaroni, G., Forastiere, F., Weinmayr, G., Jaensch, A., Nagel, G., Concin, H., and Spadaro, J. V.: Global estimates of mortality associated with long-term exposure to outdoor fine particulate matter, PNAS, 115, 9592-9597, https://doi.org/10.1073/pnas.1803222115, 2018.

Calvert, J. G. and Stockwell, W. R.: Acid generation in the troposphere by gas-phase chemistry, Environ. Sci. Technol., 17, 428A-443A, https://doi.org/10.1021/es00115a727, 1983.

Cao, J.-j., Wang, Q.-y., Chow, J. C., Watson, J. G., Tie, X.-x., Shen, Z.-x., Wang, P., and An, Z.-s.: Impacts of aerosol compositions on visibility impairment in Xi'an, China, Atmos. Environ., 59, 559-566, https://doi.org/10.1016/j.atmosenv.2012.05.036, 2012.

Cao, T., Wang, H., Chen, X., Li, L., Lu, X., Lu, K., and Fan, S.: Rapid increase in spring ozone in the Pearl River Delta, China during 2013-2022, npj Clim. Atmos. Sci., 7, 309, https://doi.org/10.1038/s41612-024-00847-3, 2024.

Carlton, A. G. and Turpin, B. J.: Particle partitioning potential of organic compounds is highest in the Eastern US and driven by anthropogenic water, Atmos. Chem. Phys., 13, 10203-10214, https://doi.org/10.5194/acp-13-10203-2013, 2013.

Chen, S.-L., Chang, S.-W., Chen, Y.-J., and Chen, H.-L.: Possible warming effect of fine particulate matter in the atmosphere, Commun. Earth Environ., 2, 208, https://doi.org/10.1038/s43247-021-00278-5, 2021.

Cheng, Z., Jiang, J., Chen, C., Gao, J., Wang, S., Watson, J. G., Wang, H., Deng, J., Wang, B., Zhou, M., Chow, J. C., Pitchford, M. L., and Hao, J.: Estimation of Aerosol Mass Scattering Efficiencies under High Mass Loading: Case Study for the Megacity of Shanghai, China, Environ. Sci. Technol., 49, 831-838, https://doi.org/10.1021/es504567q, 2015.

Chow, J. C., Lowenthal, D. H., Chen, L. W. A., Wang, X., and Watson, J. G.: Mass reconstruction methods for PM2.5: a review, Air Quality, Atmosphere & Health, 8, 243-263, https://doi.org/10.1007/s11869-015-0338-3, 2015.

Chow, W. S., Liao, K., Huang, X. H. H., Leung, K. F., Lau, A. K. H., and Yu, J. Z.: Measurement Report: Ten-year trend of PM2.5 major components and source tracers from 2008 to 2017 in an urban site of Hong Kong, China, Atmos. Chem. Phys., 2022, 1-24, https://doi.org/10.5194/acp-2022-100, 2022.

Urban Ambient Air Quality in Guangdong Province (2015): https://gdee.gd.gov.cn/kqzl/content/post_2301048.html, last access: 13 June 2024.

Ding, K., Huang, X., Ding, A., Wang, M., Su, H., Kerminen, V.-M., Petäjä, T., Tan, Z., Wang, Z., Zhou, D., Sun, J., Liao, H., Wang, H., Carslaw, K., Wood, R., Zuidema, P., Rosenfeld, D., Kulmala, M., Fu, C., Pöschl, U., Cheng, Y., and Andreae, M. O.: Aerosol-boundary-layer-monsoon interactions amplify semi-direct effect of biomass smoke on low cloud formation in Southeast Asia, Nat. Commun., 12, 6416, https://doi.org/10.1038/s41467-021-26728-4, 2021.

https://doi.org/10.5194/egusphere-2025-2204
Preprint. Discussion started: 28 May 2025

Duan, J., Lyu, R., Wang, Y., Xie, X., Wu, Y., Tao, J., Cheng, T., Liu, Y., Peng, Y., Zhang, R., He, Q., Ga, W., Zhang, X., and Zhang, Q.: Particle Liquid Water Content and Aerosol Acidity Acting as Indicators of Aerosol Activation Changes in Cloud Condensation Nuclei (CCN) during Pollution Eruption in Guangzhou of South China, Aerosol Air Qual. Res., 9, 2662-2670, https://doi.org/10.4209/aaqr.2019.09.0476, 2019.

https://emep-ccc.nilu.no/monitoring-program, last access: 3 December 2024.

Spatial and Seasonal Patterns and Temporal Variability of Haze and its Constituents in the United States: Report V June 2011: https://vista.cira.colostate.edu/Improve/spatial-and-seasonal-patterns-and-temporal-variability-of-haze-and-its-constituents-in-the-united-states-report-v-june-2011/, last access: 24 June 2024.

Fang, T., Guo, H. Y., Zeng, L. H., Verma, V., Nenes, A., and Weber, R. J.: Highly Acidic Ambient Particles, Soluble Metals, and Oxidative Potential: A Link between Sulfate and Aerosol Toxicity, Environ. Sci. Technol., 51, 2611-2620, https://doi.org/10.1021/acs.est.6b06151, 2017.

Finlayson-Pitts, B. J., Ezell, M. J., and Pitts, J. N.: Formation of chemically active chlorine compounds by reactions of atmospheric NaCl particles with gaseous N2O5 and ClONO2, Nature, 337, 241-244, https://doi.org/10.1038/337241a0, 1989.

Fountoukis, C. and Nenes, A.: ISORROPIA II: a computationally efficient thermodynamic equilibrium model for K+–Ca2+–Mg2+–NH4+–Na+–SO42−–NO3−–Cl−–H2O aerosols, Atmos. Chem. Phys., 7, 4639-4659, https://doi.org/10.5194/acp-7-4639-2007, 2007.

Fu, X., Guo, H., Wang, X., Ding, X., He, Q., Liu, T., and Zhang, Z.: PM2.5 acidity at a background site in the Pearl River Delta region in fall-winter of 2007–2012, J. Hazard. Mater., 286, 484-492, https://doi.org/10.1016/j.jhazmat.2015.01.022, 2015.

Fu, X., Wang, X., Hu, Q., Li, G., Ding, X., Zhang, Y., He, Q., Liu, T., Zhang, Z., Yu, Q., Shen, R., and Bi, X.: Changes in visibility with PM2.5 composition and relative humidity at a background site in the Pearl River Delta region, J. Environ. Sci., 40, 10-19, https://doi.org/10.1016/j.jes.2015.12.001, 2016.

Fu, X. X., Wang, X. M., Guo, H., Cheung, K. L., Ding, X., Zhao, X. Y., He, Q. F., Gao, B., Zhang, Z., Liu, T. Y., and Zhang, Y. L.: Trends of ambient fine particles and major chemical components in the Pearl River Delta region: Observation at a regional background site in fall and winter, Sci. Total Environ., 497, 274-281, https://doi.org/10.1016/j.scitotenv.2014.08.008, 2014.

Geng, G., Zhang, Q., Tong, D., Li, M., Zheng, Y., Wang, S., and He, K.: Chemical composition of ambient PM2. 5 over China and relationship to precursor emissions during 2005–2012, Atmos. Chem. Phys., 17, 9187-9203, https://doi.org/10.5194/acp-17-9187-2017, 2017.

Geng, G., Liu, Y., Liu, Y., Liu, S., Cheng, J., Yan, L., Wu, N., Hu, H., Tong, D., Zheng, B., Yin, Z., He, K., and Zhang, Q.: Efficacy of China's clean air actions to tackle PM2.5 pollution between 2013 and 2020, Nat. Geosci., 17, 987-994, https://doi.org/10.1038/s41561-024-01540-z, 2024.

Geng, G. N., Xiao, Q. Y., Zheng, Y. X., Tong, D., Zhang, Y. X., Zhang, X. Y., Zhang, Q., He, K. B., and Liu, Y.: Impact of China's Air Pollution Prevention and Control Action Plan on PM2.5 chemical composition over eastern China, Science China-Earth Sciences, 62, 1872-1884, https://doi.org/10.1007/s11430-018-9353-x, 2019.

Guo, Q., Wang, Y., Zheng, J., Zhu, M., Sha, Q. e., and Huang, Z.: Temporal evolution of speciated volatile organic compound (VOC) emissions from solvent use sources in the Pearl River Delta Region, China (2006–2019), Sci. Total Environ., 933, 172888, https://doi.org/10.1016/j.scitotenv.2024.172888, 2024.

Gwynn, R. C., Burnett, R. T., and Thurston, G. D.: A time-series analysis of acidic particulate matter and daily mortality and morbidity in the Buffalo, New York, region, Environ. Health Perspect., 108, 125-133, https://doi.org/10.1289/ehp.00108125, 2000.

A Concise Guide to the Air Pollution Control Ordinance: https://www.epd.gov.hk/epd/english/environmentinhk/air/guide_ref/guide_apco.html#introduction, last access: 3 December 2024.

https://doi.org/10.5194/egusphere-2025-2204
Preprint. Discussion started: 28 May 2025

Jung, J., Lee, H., Kim, Y. J., Liu, X., Zhang, Y., Gu, J., and Fan, S.: Aerosol chemistry and the effect of aerosol water content on visibility impairment and radiative forcing in Guangzhou during the 2006 Pearl River Delta campaign, J. Environ. Manage., 90, 3231-3244, https://doi.org/10.1016/j.jenvman.2009.04.021, 2009.

Kang, H. G., Kim, Y., Collier, S., Zhang, Q., and Kim, H.: Volatility of Springtime ambient organic aerosol derived with thermodenuder aerosol mass spectrometry in Seoul, Korea, Environ. Pollut., 304, 119203, https://doi.org/10.1016/j.envpol.2022.119203, 2022.

Kawamura, K. and Bikkina, S.: A review of dicarboxylic acids and related compounds in atmospheric aerosols: Molecular distributions, sources and transformation, Atmos. Res., 170, 140-160, https://doi.org/10.1016/j.atmosres.2015.11.018, 2016.

Kim, W., Lee, H., Kim, J., Jeong, U., and Kweon, J.: Estimation of seasonal diurnal variations in primary and secondary organic carbon concentrations in the urban atmosphere: EC tracer and multiple regression approaches, Atmos. Environ., 56, 101-108, https://doi.org/10.1016/j.atmosenv.2012.03.076, 2012.

Li, J., Zhang, Z., Wu, Y., Tao, J., Xia, Y., Wang, C., and Zhang, R.: Effects of chemical compositions in fine particles and their identified sources on hygroscopic growth factor during dry season in urban Guangzhou of South China, Sci. Total Environ., 801, 149749, https://doi.org/10.1016/j.scitotenv.2021.149749, 2021.

Li, Y., Lei, L., Sun, J., Gao, Y., Wang, P., Wang, S., Zhang, Z., Du, A., Li, Z., Wang, Z., Kim, J. Y., Kim, H., Zhang, H., and Sun, Y.: Significant Reductions in Secondary Aerosols after the Three-Year Action Plan in Beijing Summer, Environ. Sci. Technol., 57, 15945-15955, https://doi.org/10.1021/acs.est.3c02417, 2023.

Liao, K., Wang, Q., Wang, S., and Yu, J. Z.: Bayesian Inference Approach to Quantify Primary and Secondary Organic Carbon in Fine Particulate Matter Using Major Species Measurements, Environ. Sci. Technol., 57, 5169-5179, https://doi.org/10.1021/acs.est.2c09412, 2023.

Liu, L., Kuang, Y., Zhai, M. M., Xue, B., He, Y., Tao, J., Luo, B., Xu, W. Y., Tao, J. C., Yin, C. Q., Li, F., Xu, H. B., Deng, T., Deng, X. J., Tan, H. B., and Shao, M.: Strong light scattering of highly oxygenated organic aerosols impacts significantly on visibility degradation, Atmos. Chem. Phys., 22, 7713-7726, https://doi.org/10.5194/acp-22-7713-2022, 2022.

Liu, M., Song, Y., Zhou, T., Xu, Z., Yan, C., Zheng, M., Wu, Z., Hu, M., Wu, Y., and Zhu, T.: Fine particle pH during severe haze episodes in northern China, Geophys. Res. Lett., 44, 5213-5221, https://doi.org/10.1002/2017GL073210, 2017.

Liu, P., Chen, H., Song, Y., Xue, C., Ye, C., Zhao, X., Zhang, C., Liu, J., and Mu, Y.: Atmospheric ammonia in the rural North China Plain during wintertime: Variations, sources, and implications for HONO heterogeneous formation, Sci. Total Environ., 861, 160768, https://doi.org/10.1016/j.scitotenv.2022.160768, 2023.

Liu, T. Y., Chan, A. W. H., and Abbatt, J. P. D.: Multiphase Oxidation of Sulfur Dioxide in Aerosol Particles: Implications for Sulfate Formation in Polluted Environments, Environ. Sci. Technol., 55, 4227-4242, https://doi.org/10.1021/acs.est.0c06496, 2021.

Luo, L., Zhang, Y.-Y., Xiao, H.-Y., Xiao, H.-W., Zheng, N.-J., Zhang, Z.-Y., Xie, Y.-J., and Liu, C.: Spatial Distributions and Sources of Inorganic Chlorine in PM2.5 across China in Winter, Atmosphere, 10, 505, 2019.

Ma, F., Wang, H., Ding, Y., Zhang, S., Wu, G., Li, Y., Gong, D., Ristovski, Z., He, C., and Wang, B.: Amplified Secondary Organic Aerosol Formation Induced by Anthropogenic–Biogenic Interactions in Forests Around Megacities, J. Geophys. Res.: Atmos., 129, e2024JD041679, https://doi.org/10.1029/2024JD041679, 2024.

Ming, L., Jin, L., Li, J., Fu, P., Yang, W., Liu, D., Zhang, G., Wang, Z., and Li, X.: PM2.5 in the Yangtze River Delta, China: Chemical compositions, seasonal variations, and regional pollution events, Environ. Pollut., 223, 200-212, https://doi.org/10.1016/j.envpol.2017.01.013, 2017.

Nenes, A., Pandis, S. N., Weber, R. J., and Russell, A.: Aerosol pH and liquid water content determine when particulate matter is sensitive to ammonia and nitrate availability, Atmos. Chem. Phys., 20, 3249-3258, https://doi.org/10.5194/acp-20-3249-2020, 2020.

Nenes, A., Pandis, S. N., Kanakidou, M., Russell, A. G., Song, S., Vasilakos, P., and Weber, R. J.: Aerosol acidity and liquid water content regulate the dry deposition of inorganic reactive nitrogen, Atmos. Chem. Phys., 21, 6023-6033, https://doi.org/10.5194/acp-21-6023-2021, 2021.

https://doi.org/10.5194/egusphere-2025-2204
Preprint. Discussion started: 28 May 2025

Nguyen, T. K. V., Zhang, Q., Jimenez, J. L., Pike, M., and Carlton, A. G.: Liquid Water: Ubiquitous Contributor to Aerosol Mass, Environ. Sci. Technol. Lett., 3, 257-263, https://doi.org/10.1021/acs.estlett.6b00167, 2016.

Pye, H. O. T., Ward-Caviness, C. K., Murphy, B. N., Appel, K. W., and Seltzer, K. M.: Secondary organic aerosol association with cardiorespiratory disease mortality in the United States, Nat. Commun., 12, 7215, https://doi.org/10.1038/s41467-021-27484-1, 2021.

Pye, H. O. T., Nenes, A., Alexander, B., Ault, A. P., Barth, M. C., Clegg, S. L., Collett Jr, J. L., Fahey, K. M., Hennigan, C. J., Herrmann, H., Kanakidou, M., Kelly, J. T., Ku, I. T., McNeill, V. F., Riemer, N., Schaefer, T., Shi, G., Tilgner, A., Walker, J. T., Wang, T., Weber, R., Xing, J., Zaveri, R. A., and Zuend, A.: The acidity of atmospheric particles and clouds, Atmos. Chem. Phys., 20, 4809-4888, https://doi.org/10.5194/acp-20-4809-2020, 2020.

Qu, Z., Henze, D. K., Capps, S. L., Wang, Y., Xu, X., Wang, J., and Keller, M.: Monthly top-down NOx emissions for China (2005–2012): A hybrid inversion method and trend analysis, 122, 4600-4625, https://doi.org/10.1002/2016JD025852, 2017.

Reuter, M., Buchwitz, M., Hilboll, A., Richter, A., Schneising, O., Hilker, M., Heymann, J., Bovensmann, H., and Burrows, J. P.: Decreasing emissions of NOx relative to CO2 in East Asia inferred from satellite observations, Nat. Geosci., 7, 792-795, https://doi.org/10.1038/ngeo2257, 2014.

Seinfeld, J. H., Pandis, S. N., and Noone, K. J. J. P. T.: Atmospheric Chemistry and Physics: From Air Pollution to Climate Change, 51, 88-90, 1998.

Song, X., Wu, D., Su, Y., Li, Y., and Li, Q.: Review of health effects driven by aerosol acidity: Occurrence and implications for air pollution control, Sci. Total Environ., 955, 176839, https://doi.org/10.1016/j.scitotenv.2024.176839, 2024.

Su, H., Cheng, Y., and Pöschl, U.: New Multiphase Chemical Processes Influencing Atmospheric Aerosols, Air Quality, and Climate in the Anthropocene, Acc. Chem. Res., 53, 2034-2043, https://doi.org/10.1021/acs.accounts.0c00246, 2020.

Turpin, B. J. and Huntzicker, J. J.: Secondary formation of organic aerosol in the Los Angeles basin: A descriptive analysis of organic and elemental carbon concentrations, Atmospheric Environment. Part A. General Topics, 25, 207-215, https://doi.org/10.1016/0960-1686(91)90291-E, 1991.

Turpin, B. J. and Huntzicker, J. J.: Identification of secondary organic aerosol episodes and quantitation of primary and secondary organic aerosol concentrations during SCAQS, Atmos. Environ., 29, 3527-3544, https://doi.org/10.1016/1352-2310(94)00276-Q, 1995.

Vohra, K., Marais, E. A., Bloss, W. J., Schwartz, J., Mickley, L. J., Van Damme, M., Clarisse, L., and Coheur, P. F.: Rapid rise in premature mortality due to anthropogenic air pollution in fast-growing tropical cities from 2005 to 2018, Sci. Adv., 8, https://doi.org/10.1126/sciadv.abm4435, 2022.

Wang, G., Tao, Y., Chen, J., Liu, C., Qin, X., Li, H., Yun, L., Zhang, M., Zheng, H., Gui, H., Liu, J., Huo, J., Fu, Q., Deng, C., and Huang, K.: Quantitative Decomposition of Influencing Factors to Aerosol pH Variation over the Coasts of the South China Sea, East China Sea, and Bohai Sea, Environ. Sci. Technol. Lett., https://doi.org/10.1021/acs.estlett.2c00527, 2022a.

Wang, G. H., Zhang, R. Y., Gomez, M. E., Yang, L. X., Zamora, M. L., Hu, M., Lin, Y., Peng, J. F., Guo, S., Meng, J. J., Li, J. J., Cheng, C. L., Hu, T. F., Ren, Y. Q., Wang, Y. S., Gao, J., Cao, J. J., An, Z. S., Zhou, W. J., Li, G. H., Wang, J. Y., Tian, P. F., Marrero-Ortiz, W., Secrest, J., Du, Z. F., Zheng, J., Shang, D. J., Zeng, L. M., Shao, M., Wang, W. G., Huang, Y., Wang, Y., Zhu, Y. J., Li, Y. X., Hu, J. X., Pan, B., Cai, L., Cheng, Y. T., Ji, Y. M., Zhang, F., Rosenfeld, D., Liss, P. S., Duce, R. A., Kolb, C. E., and Molina, M. J.: Persistent sulfate formation from London Fog to Chinese haze, PNAS, 113, 13630-13635, https://doi.org/10.1073/pnas.1616540113, 2016.

Wang, J., Gao, J., Che, F., Wang, Y., Lin, P., and Zhang, Y.: Decade-long trends in chemical component properties of PM2.5 in Beijing, China (2011−2020), Sci. Total Environ., 832, 154664, https://doi.org/10.1016/j.scitotenv.2022.154664, 2022b.

Wang, S., Wang, L., Li, Y., Wang, C., Wang, W., Yin, S., and Zhang, R.: Effect of ammonia on fine-particle pH in agricultural regions of China: comparison between urban and rural sites, Atmos. Chem. Phys., 20, 2719-2734, https://doi.org/10.5194/acp-20-2719-2020, 2020.

Wang, X. M., Ding, X., Fu, X. X., He, Q. F., Wang, S. Y., Bernard, F., Zhao, X. Y., and Wu, D.: Aerosol scattering coefficients and major chemical compositions of fine particles observed at a rural site hit the central Pearl River Delta, South China, J. Environ. Sci., 24, 72-77, https://doi.org/10.1016/s1001-0742(11)60730-4, 2012.

https://doi.org/10.5194/egusphere-2025-2204
Preprint. Discussion started: 28 May 2025

595 . WHO Global Air Quality Guidelines in 2021: https://www.who.int/news-room/questions-and-answers/item/who-global-air-quality-guidelines, last access: 17 June 2024.

Wu, G., Wang, H., Zhang, C., Gong, D., Liu, X., Ristovski, Z., and Wang, B.: Anthropogenic pollutants induce enhancement of aerosol acidity at a mountainous background atmosphere in southern China, Sci. Total Environ., 903, 166192, https://doi.org/10.1016/j.scitotenv.2023.166192, 2023.

600 Yan, F. H., Chen, W. H., Jia, S. G., Zhong, B. Q., Yang, L. M., Mao, J. Y., Chang, M., Shao, M., Yuan, B., Situ, S., Wang, X. M., Chen, D. H., and Wang, X. M.: Stabilization for the secondary species contribution to PM2.5 in the Pearl River Delta (PRD) over the past decade, China: A meta-analysis, Atmos. Environ., 242, https://doi.org/10.1016/j.atmosenv.2020.117817, 2020.

Yang, K., Chen, D.-H., Ding, X., Li, J., Zhang, Y.-Q., Zhang, T., Wang, Q.-Y., Wang, J.-Q., Cheng, Q., Jiang, H., Liu, P.,
605 Wang, Z.-R., He, Y.-F., Zhang, G., and Wang, X.-M.: Different roles of primary and secondary sources in reducing PM2.5: Insights from molecular markers in Pearl River Delta, South China, Atmos. Environ., 294, 119487, https://doi.org/10.1016/j.atmosenv.2022.119487, 2023.

Yu, J. Z., Huang, X.-F., Xu, J., and Hu, M.: When Aerosol Sulfate Goes Up, So Does Oxalate: Implication for the Formation Mechanisms of Oxalate, Environ. Sci. Technol., 39, 128-133, https://doi.org/10.1021/es049559f, 2005.

610 Zhang, Q., Meng, X., Shi, S., Kan, L., Chen, R., and Kan, H.: Overview of particulate air pollution and human health in China: Evidence, challenges, and opportunities, The Innovation, 3, 100312, https://doi.org/10.1016/j.xinn.2022.100312, 2022a.

Zhang, Q., Zheng, Y. X., Tong, D., Shao, M., Wang, S. X., Zhang, Y. H., Xu, X. D., Wang, J. N., He, H., Liu, W. Q., Ding, Y. H., Lei, Y., Li, J. H., Wang, Z. F., Zhang, X. Y., Wang, Y. S., Cheng, J., Liu, Y., Shi, Q. R., Yan, L., Geng, G. N., Hong, C. P., Li, M., Liu, F., Zheng, B., Cao, J. J., Ding, A. J., Gao, J., Fu, Q. Y., Huo, J. T., Liu, B. X., Liu, Z. R., Yang, F. M.,
615 He, K. B., and Hao, J. M.: Drivers of improved PM2.5 air quality in China from 2013 to 2017, PNAS, 116, 24463-24469, https://doi.org/10.1073/pnas.1907956116, 2019.

Zhang, Q., Jimenez, J. L., Canagaratna, M. R., Allan, J. D., Coe, H., Ulbrich, I., Alfarra, M. R., Takami, A., Middlebrook, A. M., Sun, Y. L., Dzepina, K., Dunlea, E., Docherty, K., DeCarlo, P. F., Salcedo, D., Onasch, T., Jayne, J. T., Miyoshi, T., Shimono, A., Hatakeyama, S., Takegawa, N., Kondo, Y., Schneider, J., Drewnick, F., Borrmann, S., Weimer, S., Demerjian,
620 K., Williams, P., Bower, K., Bahreini, R., Cottrell, L., Griffin, R. J., Rautiainen, J., Sun, J. Y., Zhang, Y. M., and Worsnop, D. R.: Ubiquity and dominance of oxygenated species in organic aerosols in anthropogenically-influenced Northern Hemisphere midlatitudes, Geophys. Res. Lett., 34, https://doi.org/10.1029/2007gl029979, 2007.

Zhang, S., Gong, D., Wu, G., Li, Y., Ding, Y., Wang, B., and Wang, H.: Molecular characteristics and formation mechanisms of biogenic secondary organic aerosols in the mountainous background atmosphere of southern China, Atmos. Environ.,
625 329, 120540, https://doi.org/10.1016/j.atmosenv.2024.120540, 2024.

Zhang, Y.-Q., Ding, X., He, Q.-F., Wen, T.-X., Wang, J.-Q., Yang, K., Jiang, H., Cheng, Q., Liu, P., Wang, Z.-R., He, Y.-F., Hu, W.-W., Wang, Q.-Y., Xin, J.-Y., Wang, Y.-S., and Wang, X.-M.: Observational Insights into Isoprene Secondary Organic Aerosol Formation through the Epoxide Pathway at Three Urban Sites from Northern to Southern China, Environ. Sci. Technol., 56, 4795-4805, https://doi.org/10.1021/acs.est.1c06974, 2022b.

630 Zheng, B., Zhang, Q., Zhang, Y., He, K. B., Wang, K., Zheng, G. J., Duan, F. K., Ma, Y. L., and Kimoto, T.: Heterogeneous chemistry: a mechanism missing in current models to explain secondary inorganic aerosol formation during the January 2013 haze episode in North China, Atmos. Chem. Phys., 15, 2031-2049, https://doi.org/10.5194/acp-15-2031-2015, 2015.

Zhou, M., Zheng, G. J., Wang, H. L., Qiao, L. P., Zhu, S. H., Huang, D. D., An, J. Y., Lou, S. R., Tao, S. K., Wang, Q., Yan, R. S., Ma, Y. G., Chen, C. H., Cheng, Y. F., Su, H., and Huang, C.: Long-term trends and drivers of aerosol pH in eastern
635 China, Atmos. Chem. Phys., 22, 13833-13844, https://doi.org/10.5194/acp-22-13833-2022, 2022.

Zhu, C.-S., Cao, J.-J., Tsai, C.-J., Zhang, Z.-S., and Tao, J.: Biomass burning tracers in rural and urban ultrafine particles in Xi'an, China, Atmos. Pollut. Res., 8, 614-618, https://doi.org/10.1016/j.apr.2016.12.011, 2017.